Electronic Supplementary Information

The reversal of spontaneous exchange bias effect and zero-field-cooling magnetization in $La_{1.5}Sr_{0.5}Co_{1-x}Fe_xMnO_6$: the effect of Fe doping

Hongguang Zhang[1,*], Liang Xie[2,*], Xuechen Liu[1], Mengxia Xiong[1], Linlin Cao[1], and Yongtao Li[1]

[1] *Center of Advanced Functional Ceramics, College of Science, Nanjing University of Posts and Telecommunications, Nanjing 210023, P. R. China*

[2] *Department of Physics, North China University of Technology, Beijing 100144, P. R. China*

Section S1. X-ray photoelectron spectroscopy studies:

To further reveal the chemical composition and oxidation states of our prepared samples, x-ray photoelectron spectroscopy (XPS) measurements were taken. As known that, XPS is a powerful tool to investigate the electronic structure of detected elements in samples surface. But it is hard to give the accurate value of stoichiometric and oxygen content, due to limitation of probing depth (surface scale, 1~3 nm) and possible contamination of absorbed oxygen in the surface. The data given by XPS only estimates the variation tendency of relative atomic ratio with doping concentration.

Figure S1 gives the XPS survey spectra of a selected sample $La_{1.5}Sr_{0.5}Co_{0.8}Fe_{0.2}MnO_6$. The characteristic core level spectra of all elements are detected. Due to the polycrystalline nature of the material, the carbon signal persists on the sample's surface. The chemical states of Co, Fe, Mn ions were determined, which are consistent with what we analyzed in XAS spectra. The $2p_{3/2}$ peak energy of Co, and Mn for $x = 0$ is 779.8 eV and 642.1eV, respectively, indicating the mixed valence states of $Co^{3+/2+}$, and $Mn^{3+/4+}$. With increase of doping content, there is slightly energy shift toward lower energy side in Co and Mn XPS, shown in Fig. S1, implying the decrease of Mn^{4+} and Co^{3+}

The statistical results of the percentage of atomics are listed in Table S1. The estimated sample stoichiometric are approximately consistent with the nominal values. From Table S1, it shows that the variation tendency of Fe doping concentration increases in general. There is fluctuation for $x = 0.1$ and 0.4, which are basically coincidence with the fluctuation of T_{C2} with doping concentration. And this fluctuation is caused by the inhomogeneity of samples, which also affects the La content. There is an obvious change of La content between samples $x < 0.2$

and $x \geq 0.2$. The ratio of La:Sr for samples $x < 0.2$ is higher than that for $x \geq 0.2$. Coincidentally, the abrupt discrepancy in XAS and magnetic data (the negative magnetization and sign switch of SEB) also occurs at this critical concentration. We propose that inhomogeneity of samples inevitably influences the electronic structure of Fe, Co and Mo ions and their mutual magnetic interaction, leading to the negative magnetization and sign reversal of SEB effect.

Section 2. Temperature and frequency dependent ac susceptibility study

The temperature dependence of dc susceptibility in ZFC mode under different magnetic fields for $La_{1.5}Sr_{0.5}CoMnO_6$ sample shows that besides the main peak at 173 K, there is another peak around 100 K. We attributed it to a glass-like behavior, which are consistent with glassy behavior around 100 K reported by Murthy *et al.* in $La_{1.5}Sr_{0.5}CoMnO_6$ by the ac susceptibility tool [1,2]. This glassy behavior was identified as a reentrant spin glass based on the critical slowing down power law. Glassy behavior is a common feature in antisite disordered systems [3-5].

Ac susceptibility measurement techniques are a powerful technique normally used to probe for glassy behavior. In order to confirm this glassy behavior, we give the temperature dependent in-phase component (χ') and out-of-phase component (χ'') of ac susceptibility for our prepared $La_{1.5}Sr_{0.5}CoMnO_6$ sample, shown in Figure S2. The ac susceptibility was measure under ac field 1 Oe at frequency 3, 33, 323, and 723 Hz. The first peak around 170 K both in $\chi'(T)$ and $\chi''(T)$ is independent with frequency, manifesting the ferromagnetic transition. A clear frequency dependence of the peak around 80 - 100 K and its shift toward higher temperature with the increase of frequency suggest the reentrant glassy dynamics. For further study this signature of reentrant glassy state, the relaxation time (τ) with the freezing

temperature T_f has been analyzed by the critical slowing down power law [6,7]. The τ vs T_f data is shown in the inset of Fig. S2, which was fitted by the power law $\tau = \tau_0 (T_f/T_g\text{-}1)^{-zv}$, where τ_0 is the microscopic spin relaxation time, T_g denotes glassy freezing temperature and zv is the critical exponent. From the fitting, the value of zv is 8.9, close to the values (5~10) for the typical spin glass system [8]. The fitted value of τ_0 is 6.1×10^{-4} s, higher than the range (10^{-10}-10^{-13} sec) of a conventional spin glass system [9]. The higher value of τ_0 implying that the spin relaxation is slower and the reentrant spin glass phases are formed by frustrated magnetized clusters instead of the individual atomic spins [10]. Most recently, this kinds of reentrant spin glass were also studied in antisite-disordered nanometric $La_{1.5}Ca_{0.5}CoMnO_6$ double perovskite [11], while an reentrant cluster glass behavior in La2CoMnO6 by analyzing the frequency dependence of ac susceptibility based the critical slowing down mode [12]. Therefore, the magnetic behavior at round 100 K is a reentrant spin glass state and that at round 170 K is a ferromagnetic transition.

Section 3. The isothermal magnetization with n-type and p-type protocol study

Figure S3 gives the virgin curve in ZFC M(H) curve and n-type and p-type ZFC M(H) curves. It is noticed that the virgin magnetization curve at T = 5 K in Fe doped samples, no matter in p-type and in n-type protocols, falls outside the M(H) hysteresis envelop up to a certain field, except the curves in the two end compounds. Some of them basically fall outside the hysteresis envelop even up to the maximum external magnetic field (±6T). The virgin magnetization increases nearly linear up to the certain field. This feature is discussed to be analogous to the field induced metamagnetic transition from canted antiferromagnetic to ferromagnetic phase observed in phase separated systems [2,13].

It is clear that the p-type and n-type M(H) loops are almost symmetric in nature, especially for the sample $x \leq 0.2$, indicating the intrinsic spontaneous exchange bias effect. for x =1 sample, the both n-type and p-type M(H) loops completely overlap together with well centrosymmetric about the origin point means the absence of ZEB effect. For samples 1 > x > 0.2, the H_{EB} does not change into negative value in the n type M(H) loops from the positive value in p-type M(H) loops. However, the diversity between these two types M(H) loops are clearly observed, showing a certain of EB effect. Actually, it can be seen that the absolute value of H_{EB} in n-type loops are to some extend larger than that in p-type measurement, which illustrates that there is a pinned intrinsic positive H_{EB} in those samples. Those inner pinned positive H_{EB} may be caused by the complex magnetic region distribution, leading to unexpected FM/AFM spin-antiparallel interface. The much more possible magnetic interactions among three magnetic transitional metal ions provide the possibility to establish the FM/AFM spin-antiparallel interface. The inner pinned positive H_{EB} is more obvious in the sample with x > 0.2. This because that the AFM behavior dominates over FM interaction, reflected from the unsaturated magnetization (apparently near linear behavior of magnetization with field) and depressed value of coercive field. Because of the inhomogeneity distribution of magnetic ions and their magnetic interactions, the spin arrangement in partial AFM domains may be pinned by the adjacent AFM domains. Even when the opposite magnetic field exerted, the spin in those domains will not orients. Therefore, when we carried out in p-type measurement, the FM/AFM interface with antiparallel spin arrangement, causing a positive exchange bias. When applied an n-type measurement, the FM/AFM interface remains the antiparallel spin arrangement and other FM/AFM interfaces with unpinned AFM domains will spin antiparallel as well. Thus, a

relative larger positive exchange bias field is detected in n-type than in p-type.

References

1 J. K. Murthy, K. D. Chandrasekhar, H. C. Wu, H. D. Yang, J.Y. Lin, and A Venimadhav, J. Phys.: Condens. Matter, 2016, **28**, 086003.

2 J. K. Murthy, and A. Venimadhav, Appl. Phys. Lett., 2013, **103**, 252410.

3 M. T. Niemier, G. H. Bernstein, G. Csaba, A. Dingler, X. S. Hu, S. Kurtz, S. Liu, J. Nahas, W. Porod, M. Siddiq, and E. Varga, J. Phys.: Condens. Matter, 2011, **23**, 49.

4 R. C. Sahoo, D. Paladhi, P. Dasgupta, A. Poddar, R. Singh, A. Das, and T. K. Nath, Journal of Magnetism and Magnetic Materials, 2017, **428**, 86.

5 J. A. Mydosh, Spin Glasses: An Experimental Introduction (London: Taylor and Francis) 1993.

6 J. Souletie, and J. L. Tholence, Phys. Rev. B, 1985, **32**, 516.

7 R. Mathieu, D. Akahoshi, A. Asamitsu, Y. Tomioka, and Y. Tokura, Phys. Rev. Lett., 2004, **93**, 227202.

8 M. Olbrich, E. Rebollar, J. Heitz, I. Frischauf, and C. Romanin, Appl. Phys. Lett., 2008, **92**, 013901.

9 S. Chatterjee, S. Giri, S. K. De, and S. Majumdar, Phys. Rev. B, 2009, **79**, 092410.

10 R. C. Sahoo, D. Paladhi, and T. K. Nath, Journal of Magnetism and Magnetic Materials, 2017, **436**, 77.

11 J. K. Murthy, and A. Venimadhav, J. Appl. Phys., 2013, **113**, 163906.

12 P. S. R. Murthy, K. R. Priolkar, P. A. Bhobe, A. Das, P. R. Sarode, and A. K. Nigam, Journal of Magnetism and Magnetic Materials, 2010, **322**, 3704.

13 Q. H. Li, N. Li, J. Hu, Q. Han, Q. Ma, L. Ge, B. Xiao, and M. Xu, J. Appl. Phys., 2014, **116**, 033905.

Table S1. The percentages of atom of $La_{1.5}Sr_{0.5}Co_{1-x}Fe_xMnO_6$, got from XPS.

	$x = 0$	$x = 0.05$	$x = 0.1$	$x = 0.2$	$x = 0.4$	$x = 0.6$	$x = 0.8$	$x = 1$
La	8.546	8.798	7.659	12.17	12.88	12.28	13.05	12.39
Sr	7.179	6.235	7.425	6.195	5.821	6.353	6.943	6.998
Fe	0	3.124	3.091	3.538	3.493	4.089	4.036	4.875
Co	5.47	5.007	5.368	4.142	3.941	2.839	1.444	0
Mn	6.263	6.422	5.838	6.592	7.039	6.522	5.962	6.368
O	72.53	70.4	70.63	67.35	66.83	67.91	68.56	69.35

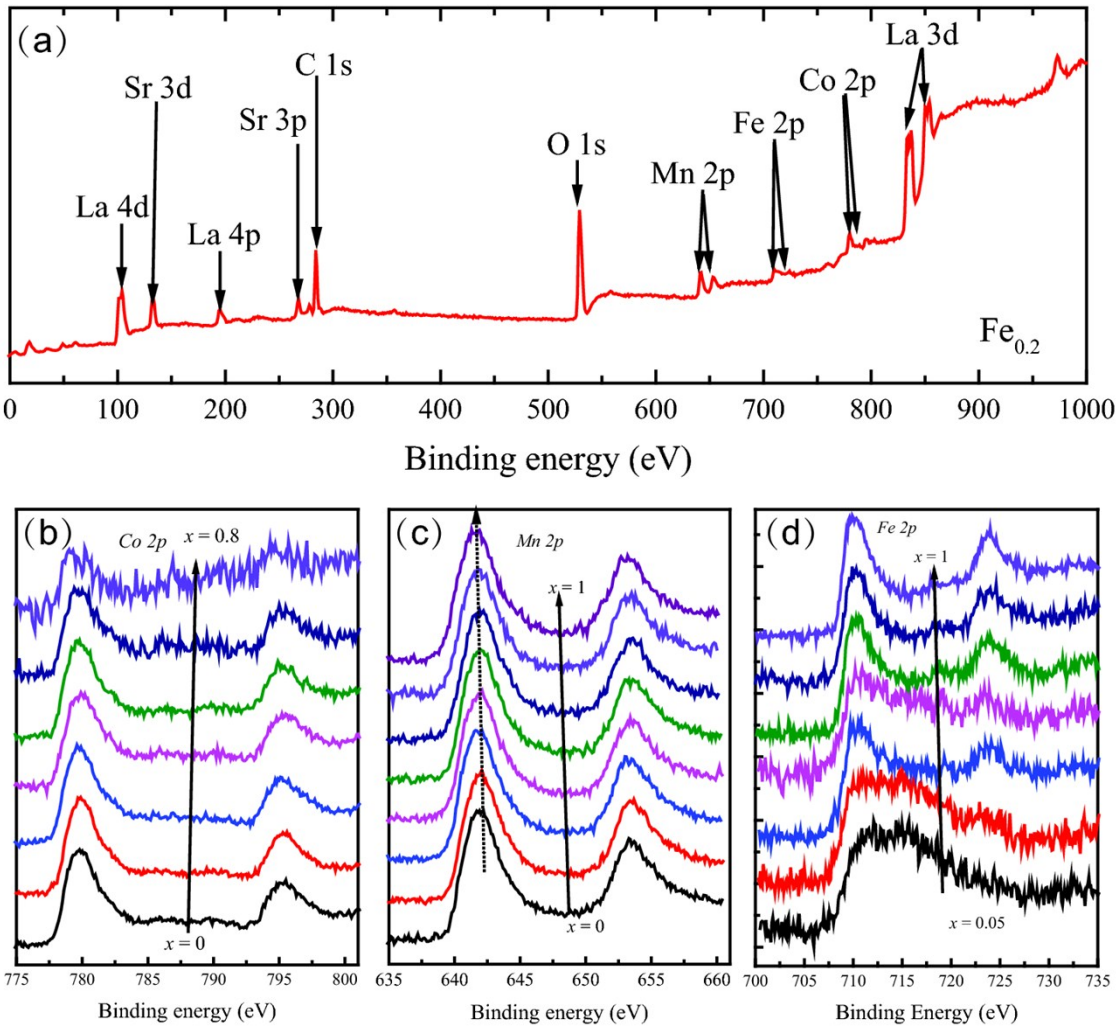

Figure S1. (a) The XPS survey spectra of a selected sample $x = 0.2$; The 2*p* core level XPS spectra of Co (b), Mn (c) and Fe (d).

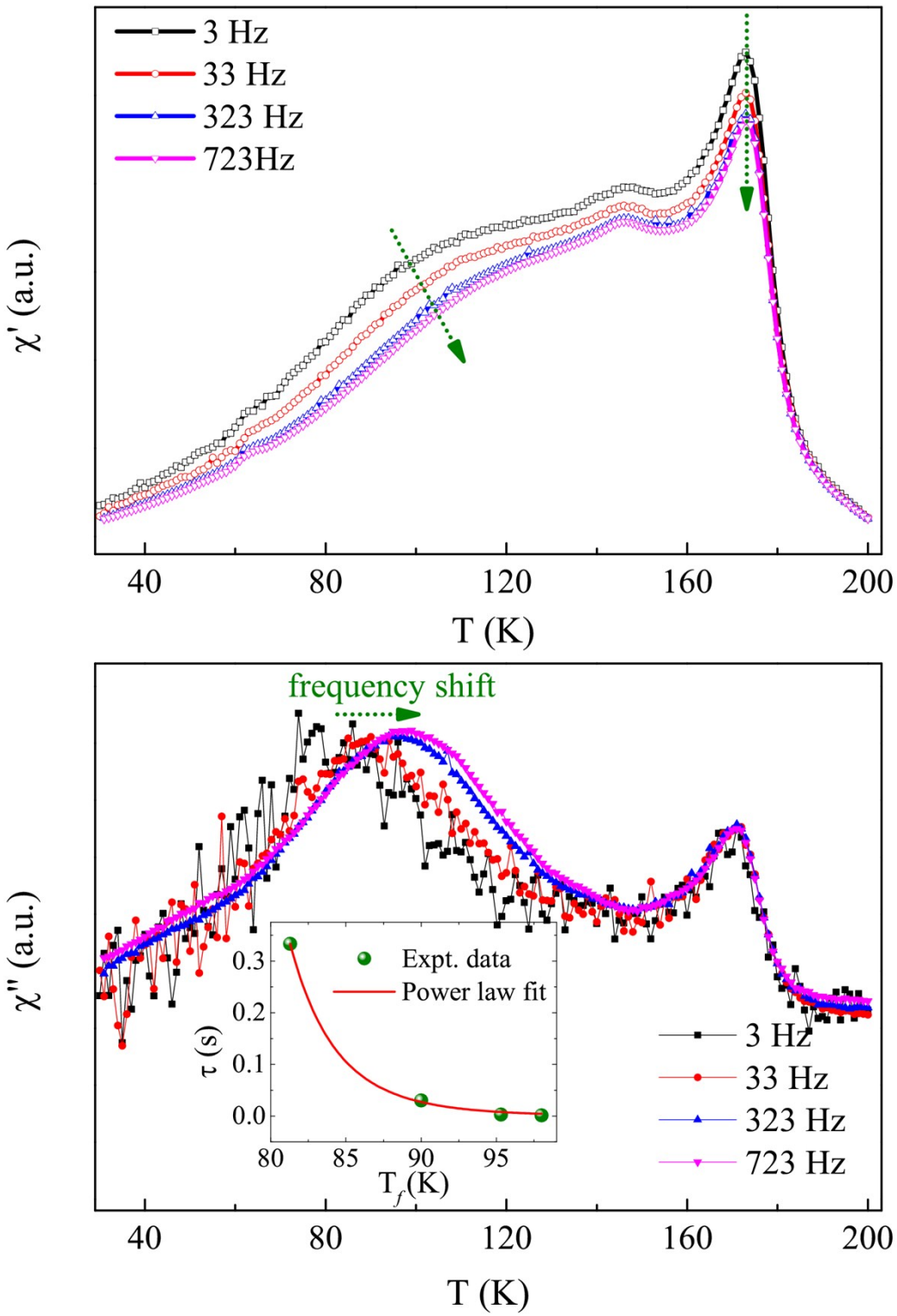

Figure S2. (a) The real-part of ac susceptibility (χ') as a function of temperature at frequency 3, 33, 323, and 723 Hz for $x = 0$; (b) The imaginary part of ac susceptibility (χ'') as a function of temperature at frequency 3, 33, 323, and 723 Hz for $x = 0$;

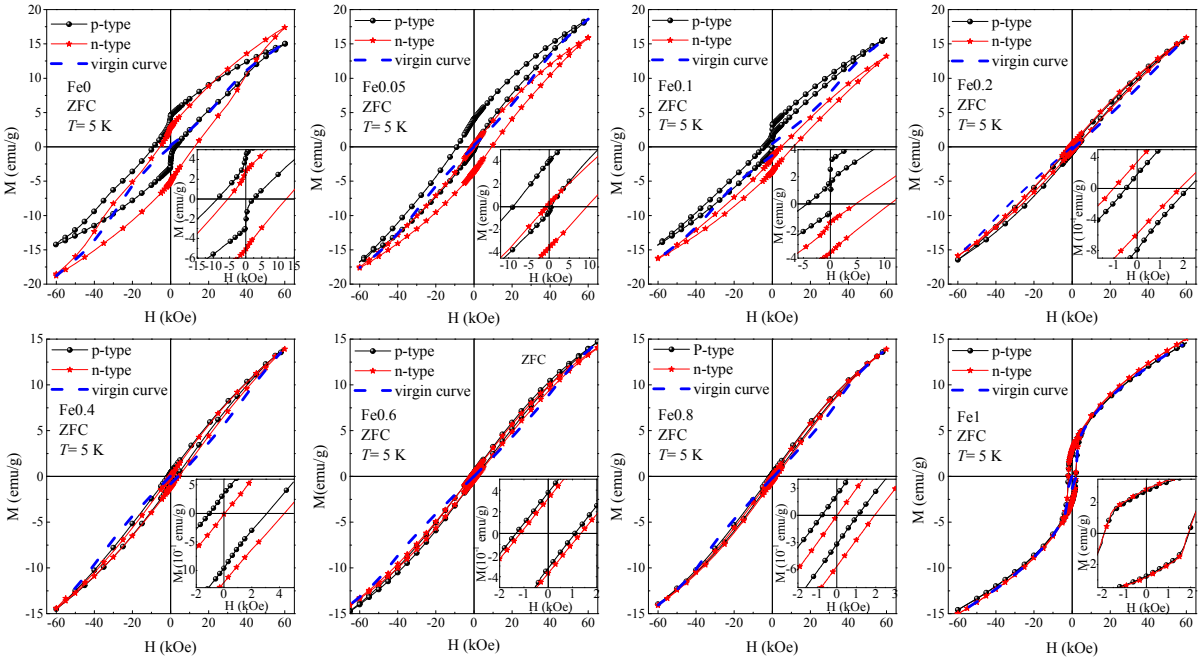

Figure S3. The virgin curve of M-H curves and M-H curves in n-type and p-type under ZFC process at T = 5 K of $La_{1.5}Sr_{0.5}Co_{1-x}Fe_xMnO_6$ (x = 0, 0.05, 0.1, 0.2, 0.4, 0.6, 0.8, and 1)